International Journal of Applied Pharmaceutics

ISSN- 0975-7058 Vol 18, Issue 2, 2026

Original Article

PREPARATION AND *IN VITRO* EVALUATION OF BUTENAFINE HCL NANOSUSPENSION

NIBRAS MAHDI NAEEM, OMAR SAEB SALIH*

Department of Pharmaceutics, College of Pharmacy, University of Baghdad, Baghdad, Iraq
***Corresponding author: Omar Saeb Salih; *Email: omar.abbas@copharm.uobaghdad.edu.iq**

Received: 04 Aug 2025, Revised and Accepted: 06 Jan 2026

ABSTRACT

Objective: One of the significant problems associated with poorly soluble drugs is low bioavailability. Butenafine HCl is classified as BCS Class II by the biopharmaceutical classification system, with low solubility and high permeability. Objectives: Formulation as a nanosuspension is an attractive and promising alternative to solve low solubility problems and low bioavailability

Methods: A nanosuspension of Butenafine HCL was generated utilizing a bottom-up method through the solvents/anti-solvents procedure characterized by particle size analysis, polydisperse index, and entrapment efficacy, and then the selected formula was described by dissolution testing, differential scanning calorimetry, X-ray powder diffraction, FTIR, and FESEM. Nanosuspensions were prepared via the solvent/anti-solvent procedure, using different polymer types and ratios.

Results: Butenafine solubilized in PBS with 1% soluplus, PVP, PEG 400, and poloxamer was 14.32±0.011, 6±0.01, 10.48±0.012, and 2.025±0.001. To form a nanosuspension with particle sizes ranging from 78 to 516 ±0.01 nm, entrapment up to 96%, and a Drug content of 99%. Particle size of optimum formula, consisting of Butenafine HCL and soluplus® in a ratio of drug: stabilizer (Soluplus®):co-stabilizer (PEG400) is (1:8:2.5) measured in nanostructure, and it was equal to 78.3±0.03 with a PDI 0.2511±0.13, which is in the nanosized range, drug content of optimum formula 99.6±0.013, and entrapment was 96±0.012. Osmolarity adjusted to a range of 280 to 310 mOsm/Kg. The release of the drug after 120 min was 95%. FTIR spectra show a distinct peak for the drug, indicating no chemical interaction between BF and Soluplus®. DSC shows a slight shift in the melting point to 220.50 °C due to the presence of cryoprotectants. PXRD shows amorphous formation due to nanosuspension, and FESEM shows the size and shape of the nanosuspension, in which the size of the particle by FESEM was 72.9 nm, which is close to the measured particle size. The stability study of the optimal formula after three months showed a particle size of 78 nm at 5 °C and 80 nm at 25 °C.

Conclusion: Using soluplus as a stabilizer at various concentrations successfully produced a nanosuspension of Butenafine HCl. The best formula, consisting of Butenafine HCL and soluplus® in a ratio of drug: stabilizer (Soluplus®):co-stabilizer (PEG400) is 1:8:2.5.

Keywords: Nanosuspension, Solubility enhancement, Antifungal, Soluplus®, Nanotechnology

DOI: https://dx.doi.org/10.22159/ijap.2026v18i2.56008 Journal homepage: https://innovareacademics.in/journals/index.php/ijap

INTRODUCTION

Fungal infections are one of the most prevalent dermatological conditions worldwide. Based on an unpublished study conducted by the International Foundation of Dermatology, superficial mycosis was among the three most commonly reported skin diseases in community-based skin disease surveys across nine countries worldwide. Human skin has favorable conditions for the growth of dermatophytes. Dermatophyte fungi invade the stratum corneum. Dermatophytes also contain serine proteinases that play a significant role in breaching the skin barrier [2]. Skin invasion entails two fundamental mechanisms: colonization and host-parasite interaction. During the colonization phase, the host initiates an immunological response, with the initial detectable immune response being cell-mediated immunity (CMI) [3]. Characterized by a pronounced inflammatory process in colonized skin. In the host-parasite contact phase, cell-mediated immunity (CMI) primarily induces disease characterized by acute inflammatory dermatophytosis, resulting in erythema and edema of the dermis and epidermis, ultimately compromising epidermal integrity [4]. Fungal keratitis is a severe infectious corneal disease that leads to corneal stromal destruction, corneal perforation, and endophthalmitis [5].

The incidence and prevalence of Fungal keratitis are gradually increasing, particularly in developing countries and tropical and subtropical regions, where Fungal keratitis accounts for approximately 50 % of all culture-positive cases of infective keratitis [6].

Nanosuspensions (NS) are submicron colloidal suspensions stabilized using surfactants. NS has many advantages over other drug delivery systems. The main advantage of NS is the enhancement of active pharmaceutical ingredient bioavailability by increasing the saturation solubility and dissolution of the active substance, and then increasing drug absorption [7, 8]. Addressing the unresolved issues related to the bioavailability of drugs categorized under the biopharmaceutical specification class II, which are characterized by limited solubility [9, 10].

Butenafine HCL is an FDA-approved drug that chemically consists of benzyl amine and naphthalene with a molecular weight of 353.93 g/mol and formula C23H27NHCl; its chemical structure is shown in fig. 1. It belongs to the class of broad-spectrum antifungal agents and inhibits the growth of fungi that produce ergosterol, an essential mediator in the formation of fungal cell membranes. Butenafine HCL exhibits inadequate oral bioavailability, with just 1.5–3% of the oral dosage detectable in the plasma one hour following a single oral administration. Butenafine HCL undergoes extensive hepatic metabolism (methylation, dealkylation, and hydroxylation), with just 0.03% of the oral dosage recovered intact from the plasma after 4 h. [11]. This aligns with the concentrations of its primary metabolite (1-naphthoic acid) in the plasma. Butenafine hydrochloride is slightly soluble in water, so we use the hydrochloride salt because it's less irritating than Butenafine itself [12].

This study aims to enhance the solubility and bioavailability of Butenafine HCL, and in future research, we formulate Butenafine HCL nanosuspension as an in-situ gel and focus on the study of the antifungal activity.

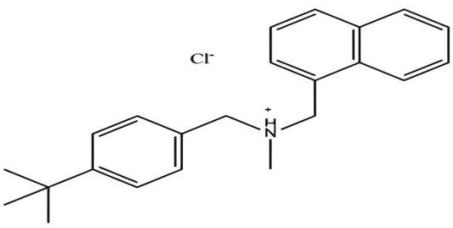

Fig. 1: Chemical structure of butenafine HCL

MATERIALS AND METHODS

Material

Butenafine HCL Powder Hangzhou, Hyperchem, China, polyvinyl caprolactam, polyvinyl acetate. Obtain from BASF (Germany), polyvinyl pyrrolidone (PVP) from Thomas Baker (Chemicals), Mumbai, India, and polyethylene glycol 400 from Alpha Chemika, India, and poloxamer 188 from MACLEAN-China.

Methods

Selection of polymer and surfactant

The selection of surfactants for nanosuspension formulation was determined by the criteria of maximum solubility of Butenafine HCL in the tested surfactants. The concentration of surfactant used for solubility testing surfactants was 1% in phosphate buffer saline, pH 6.8, for (PVP, Poloxamer188**,** Soluplus®, and PEG) [13].

The design of experiment (DoE)

The Design of Experiments is a statistical optimization technique used to evaluate the effects of formulation variables on the selection of an optimized formula [14]. In the last 20 y, opinions on ensuring the quality of pharmaceutical products and achieving the most appropriate formulation have gained prominence in the pharmaceutical industry. The effects of critical formulation and/or process parameters can be determined by optimizing formulation and/or process requirements using a design of experiments (DoE), one such approach. Therefore, the effects of independent variables, which are thought to be effective in the formulation, on the dependent variables can be successfully investigated experimentally [15]. The type used for DOE was the Response Surface (Box-Behnken Design, BBD) version 12. The factor was polymer concentration, with a minimum value of 3 times the drug concentration and a maximum of 8 times the drug concentration. The ratio selection is based on a pre-formulation study. The resulting particle size was selected based on the T-test.

Preparation of butenafine HCL nanosuspension

A nanosuspension of Butenafine HCL was generated utilizing a bottom-up method through the solvents/anti-solvents procedure. The experimental design for the nanosuspension employed a complete factorial design in accordance with the principles of Design of Experiments (DoE). The 200 mg BF was dissolved in 3 ml of methanol, yielding a solvent system. The anti-solvent system consisted of 20 ml of phosphate-buffered saline (pH 6.8) and various stabilizer and co-stabilizer ratios and types, as shown in table 1. The surfactant ratios used in the preparation of the nanosuspension, according to the results obtained from DOE, were 3%, 5.5%, and 8%. The suitable co-stabilizer used was Polyethylene glycol. The organic phase was introduced dropwise via a needle using a plastic syringe into a stabilizer solution at room temperature (25±10 °C). After the addition of the organic solvent, the mixture was stirred at 1000 rpm using a magnetic stirrer for 1 h to ensure efficient solvent evaporation. No sonication was used because the heat generated by sonication would disrupt the nanoparticles.

Characterization of the prepared butenafine HCL nanosuspension

Particle Size (PS) and polydispersity index (PDI)

At room temperature, the size and distribution of butenafine HCl nanosuspensions in all formulations were measured using a Nano-Laser particle size analyzer (Malvern Zetasizer, Ultra-Rate Company, USA) employing dynamic light scattering (DLS). Particle size (PS) and polydispersity index (PDI) are both evaluated [18-21].

Table 1: Composition of butenafine HCl nanosuspension formulation

Formula symbol	Ratio of drug: stabilizer: co-stabilizer (PEG400)	Type of stabilizer
F1	1:3:3	PVP
F2	1:3:2	PVP
F3	1:3:1	PVP
F4	1:3:3	Soluplus®
F5	1:3:1	Poloxamer188
F6	1:3:2.5	Poloxamer188
F7	1:3:1.5	Soluplus®
F8	1:3:2.5	Soluplus®
F9	1:3:1.5	Poloxamer188
F10	1:5.5:1	PVP
F11	1:5.5:2	PVP
F12	1:5.5:3	PVP
F13	1:8:2.5	Soluplus®
F14	1:8:1.5	Poloxamer188
F15	1:8:2	PVP
F16	1:8:3	PVP
F17	1:8:3	Poloxamer188
F18	1:8:1	Soluplus®

Drug content

A suitable volume of drug-loaded nanosuspension, about 1 ml of selected formula, was then diluted to 10 ml of methanol after a series of dilutions. The drug content was obtained by measuring the absorbance at 288 nm using a UV spectrophotometer, and the amount of drug was calculated using the equation Y=0.0267X-0.049, R^2=0.998 [22-25].

Entrapment efficiency measurement of the produced butenafine HCL

Nanosuspension

Utilizing the indirect method to calculate the entrapment, the produced Butenafine HCL nanosuspension formulation was separated into Amicon. The sample was then centrifuged for 30 min ±1 min at 4000 rpm to assess the entrapment efficiency and determine the quantity of drug incorporated into the nanoparticles. The amount of medication was analyzed spectrophotometrically using a UV light spectrophotometer, with absorbance measured at 288 nm. The calibration curve of Butenafine HCL in phosphate buffer saline had been used to determine the quantity of Butenafine HCL [26]. Depend on calibration equation Y=0.0023X-0.0195 with R^2=0.9985.

$$EE\% = \frac{(\text{Total drug in formula} - \text{Amount of free drug})}{\text{Total drug in formula}} \times 100\% \text{ [27] ..... eq. (1)}$$

In vitro dissolution study

The formulas with the smallest particle size and PDI, higher EE%, and the highest drug content % have been selected for *in vitro* release using dissolution apparatus type II 5 5 ml of nanosuspension preparation was inserted into the dialysis bag (12000-14000 Da

presoaked for the entire night in phosphate buffer saline, pH 6.8. The bag was closed at both ends and immersed in 900 ml phosphate-buffered saline (pH 6.8), then rotated at 50 rpm at 37 ±1 °C on a hot plate. 5 ml of the sample was taken out and replaced with fresh dissolution media at 5,10,15,30,45,60,90 min, The samples were measured spectrophotometrically at 288 nm, and this equation measured the amount of drug release: Y=0.0013X-0.0195 with R2=0.9985 [28].

Membrane filtration is performed using a 0.24µm filter syringe and repeated in triplicate. The dissolution test outcomes were statistically validated using the similarity factor (f2) to compare the release profiles of the pure drug and the selected formulation.

$$f_2 = 50 \times \log \{[1+(1/n) \sum_{j=1}^{n} w|R_j - T_j^{2.5} \times 100\} \ldots\ldots\ldots \text{eq (2)}$$

The similar factor ranges from 0 to 100. An f_2 value of 50 signifies a comparable disintegration profile, whereas a value below 50 shows dissimilar profiles [29-33].

The *in vitro* release kinetics of butenafine HCl from the prepared nanosuspension formulation were evaluated to characterize the drug release behavior. The coefficient of determination (R^2) was computed from the linear regression of these plots.

Osmolarity measurement and adjustment

The pH of the formulation is crucial to prevent irritation and side effects. The osmolarity of the nanosuspension was measured using a freezing-point depression osmometer. This method determines the total osmolality in aqueous solutions and requires only small sample volumes. By comparing the freezing points of pure water and the solution, the total osmolality is established. While water freezes at 0 °C, a solution with a salt concentration of 1 osmol/kg freezes at −1.858 °C. The measuring range is 0 to 3000 mol/kg H2O. Approximately 50 µl** of the test sample was placed into the measuring vessel, and after attaching the boat to the thermistor, the probe was inserted into the freezing chamber. The ship was subjected to freezing, and the resultant osmolarity was measured and displayed digitally [34, 35].

Freeze-drying of the prepared formulation

Freeze-drying was used to convert the optimum formula to dry powder. Mannitol is used as a cryoprotectant at 2% w/v. Approximately 40 ml of the optimized formulation was collected and freeze-dried to yield a dry powder for analysis.

Differential scanning calorimetric (DSC)

Device for measuring heat transfer (DSC-60) made by Shimadzu in Japan. The temperature of the instrument was increased from 25 to 300 °C at a heating rate of 10 °C/min, with a nitrogen flow rate of 50 ml/min. Shimadzu® Co. supplied the software (TA-60WS) version 2.2 for data collection and analysis, which was used to generate and analyze the thermograms [36].

Powder X-ray diffraction (PXRD)

The crystalline composition of the lyophilized nanosuspension powder of Butenafine HCl was analyzed using powder X-ray diffraction (XRD; Shimadzu XRD-6000, Japan). Measurements were performed using a Cu Kα filter at 40 kV and 30 mA. The scanning was conducted within a 2θ range of 2θ to 80θ [37].

Fourier transform infrared spectroscopy (FTIR)

FTIR scanning of KBr pellets containing powder samples of Butenafine HCL, lyophilized formulas in the wave number range 400-4000 at a resolution of 4 cm-1, with a speed of 2 mm/sec [38-40]

Field emission-scanning electron microscope (FESEM)

A Monitor 50 FEI field emission scanning electron microscope (FESEM) was employed to examine the surface morphology of the Butenafine HCL. The samples were analyzed at different magnification powers, and high-resolution photographs were recorded into a computer for subsequent processing. The Butenafine HCL nanosuspension was uniformly applied to double-sided adhesive carbon tapes, which were subsequently attached to FESEM specimen mounts. A sputter coating process was conducted for 2 min±1 min before imaging to provide a homogeneous coating on the samples. This procedure entailed the application of a thin coating layer on the specimens to improve conductivity and boost imaging quality [41].

Stability study

Physical stability of the optimized nanosuspension was evaluated for a period of up to 3 mo (In this article, we made efforts for the preparation of nano-scale nanosuspension, we justified osmolarity, ocular irritation for future work) at 25 °C±1 °C and 5 °C±1 °C. Nanosuspension was stored in a closed, glass vial. The stability was assessed in terms of particle size and drug content [42].

RESULTS AND DISCUSSION

Selection of polymer and surfactant

Based on the reproducible results of DOE and the solubility of Butenafine HCL with 1% of the polymer in the PBS at (pH 6.8) to get sink condition and the ability to inhibit crystal growth, a suitable polymer was selected [43].

The table (2) shows the Solubility of Butenafine HCL in the PBS at pH 6.8 with different types of polymers.

Table 2: Saturated solubility of butenafine HCL in phosphate buffer saline with 1% surfactant (pH 6.8)

Term	PBS with 1% soluplus® (mg/ml)	PBS with 1% PVP (mg/ml)	PBS with 1% PEG400 (mg/ml)	PBS with 1% poloxamer (mg/ml)
Pure BF HCl	14.32 ±0.011	6.08±0.01	10.46 ±0.012	2.025±0.001

Data are given as mean±SD; n = 3

Optimum formula by DOE

Design is a current tool for optimizing the overall number of connected components and finding critical process parameters utilizing design of experiments (DOE), interaction impact on PS, and PDI. After running order randomization, the nanosuspension for each experimental run was prepared in triplicate according to its actual composition, and then it was analyzed for PS and PDI. According to the data in table 3, DOE chooses the best formula based on the concentration of the inputs.

Table 3: Desirability, predictability, and measured PS of optimum formula by DOE

Formula code	Ratio of drug: stabilizer: co-stabilizer (PEG400)	Type of stabilizer	Desirability	Predictable PSnm	Measured PSnm
F4	1:3:3	Soluplus®	0.701	80.3 nm	88.89 nm
F7	1:3:1.5	Soluplus®	0.612	120.4 nm	137.3 nm
F8	1:3:2.5	Soluplus®	0.678	90.21 nm	110.5 nm
F13	1:8:2.5	Soluplus®	1	76.8 nm	78.3 nm
F18	1:8:1	Soluplus®	0.912	82.45 nm	89.22 nm

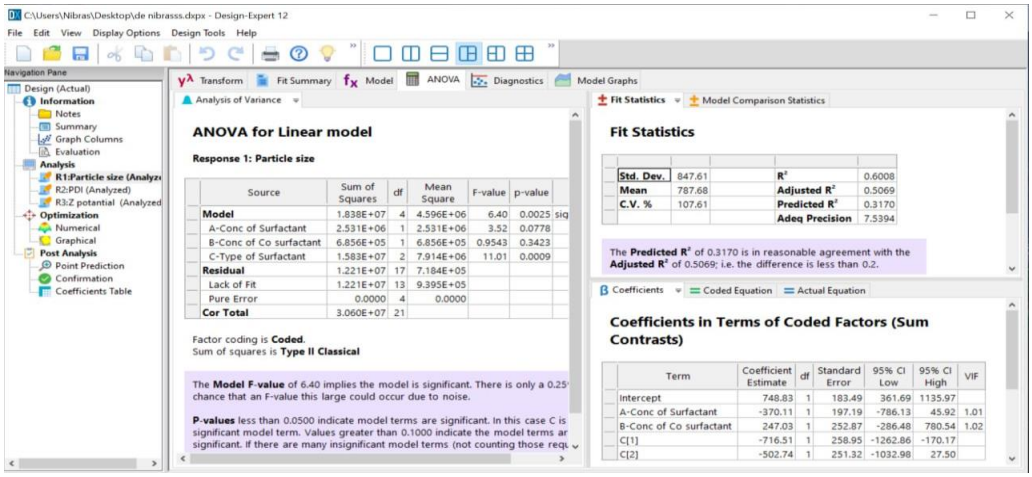

Fig. 2: ANOVA table of DOE

Particle size (PS) and polydispersity index (PDI)

Particle size and PDI measurements are the most critical characterization parameters for the prepared NS. The average particle size and PDI, which govern the physicochemical properties like saturation solubility, dissolution velocity, and physical stability [44]. Nanosuspension is a colloidal dispersion having a particle size range between 1 and 1,000 nm. A PDI value of (0.1–0.25) indicates a narrow size distribution, and a PDI value above 0.5 indicates a broad distribution [42]. As illustrated in table 4, the impact of P. S. and PDI was examined across 18 different formulations. Most of the formulations showed nano-scale particle sizes, as shown in table 4. When we use PVP as a stabilizer in (F1, F2, and F3) at low concentration with different ratios of co-stabilizer, the particle size average was (493.4 nm, 615.3 nm, and 645 nm), respectively. As the PVP concentration increases, the particle size decreases to 350 nm, as shown in (F10). Still, the further increase in concentration of PVP increases the PS, as shown in (F15 and F16), as shown in table 4. PVP, used as a nonionic polymer, played a significant role in the size-reduction process. PVP has a relatively low molecular weight; thus, it forms small particles faster. One of the main mechanisms of stabilizer-induced inhibition of aggregation and agglomeration is the formation of a steric barrier around the particles [45]. At low concentration, as in (F1, F2, and F3), it appears that the concentration was not sufficient to cover the surfaces of Butenafine particles completely. As the concentration of PVP increased, as shown in (F10, F11, and F12), the Butenafine particles were entirely covered by PVP, which increases the adsorption capacity on the particle surface. At higher concentrations (F15 and F16), the particle size of the nanosuspension increased. This shift is attributed to two reasons. Firstly, at high PVP concentrations above the critical micelle concentration (CMC), micelles form and play a vital role in the thermal instability of nanosuspensions. However, the formed micelles could compete with monomers for adsorption at the drug surface, leading to decreased total interfacial adsorption and, hence, particle size enlargement. Secondly, it causes the thickening of the particle coating and inhibits the diffusion between the solvent and anti-solvent during precipitation [46].

Soluplus® formulas exhibit smaller PS and a more uniform size distribution. Soluplus® exhibits superior wettability and steric stabilization compared to other polymeric stabilizers, which is attributed to its bifunctional properties and the large size of its molecule. Soluplus® is an amphipathic graft copolymer that contains a hydrophilic part (polyethylene glycol backbone) and a lipophilic part (vinyl caprolactam/vinyl acetate side chain). The adsorption of Soluplus® onto drug particles decreases the interfacial tension at the particle surface, thereby providing steric hindrance that prevents aggregation of the newly formed nanoparticles. The best Butenafine HCL-Soluplus® ratio was shown in (F13) because it had the smallest particle size and PDI value [47-49].

In the case of Poloxamer 188 as the stabilizer, the particle size was outside the normal nano-size range observed in F5 and F6, with a high PDI. This indicates that this combination (poloxamer 188: PEG400) was not suitable for Butenafine nanosuspension. Nanosuspension was prepared using PEG400 as a co-stabilizer. The results showed that increasing the PEG400 concentration decreased particle size and PDI, resulting in more uniformly distributed particles.

Table 4: PS and PDI of butenafine HCL nanosuspension formulas

Formula code	Ratio of drug: stabilizer: co-stabilizer (PEG400)	Type of stabilizer	Particle size (PS) ±SD	Polydispersity index (PDI) ±SD
F1	1:3:3	PVP	493.4±0.01	0.7368±0.02
F2	1:3:2	PVP	615.3±0.01	1.029±0.0012
F3	1:3:1	PVP	645±0.02	1.032±0.03
F4	1:3:3	Soluplus®	88.89±0.012	0.3021±0.012
F5	1:3:1	Poloxamer188	>1000	1.393±0.013
F6	1:3:2.5	Poloxamer188	>1000	1.639±0.03
F7	1:3:1.5	Soluplus®	137.3±0.01	0.2689±0.013
F8	1:3:2.5	Soluplus®	110.5±0.01	0.3243±0.02
F9	1:3:1.5	Poloxamer188	842.6±0.01	1.026±0.01
F10	1:5.5:1	PVP	350.08±0.12	0.1495±0.01
F11	1:5.5:2	PVP	116.3±0.02	0.425±0.02
F12	1:5.5:3	PVP	84.49±0.11	0.2751±0.012
F13	1:8:2.5	Soluplus®	78.3±0.03	0.2511±0.13
F14	1:8:1.5	Poloxamer188	1336±0.13	1.098±0.01
F15	1:8:2	PVP	299.2±0.01	0.4851±0.14
F16	1:8:3	PVP	297.1±0.02	0.537±0.15
F17	1:8:3	Poloxamer188	516.6±0.12	0.478±0.02
F18	1:8:1	Soluplus®	89.22±0.13	0.3391±0.3

n=3

Drug content and entrapment efficacy (EE)

According to PS and DOE, the optimum formulation was selected, and we measured the Drug content EE. The drug content of the formulated nanosuspension was found to be in the range of 90% to 99%, respectively, as shown in table 5. Formulation F13 showed the maximum drug content, i. e., 99%, in which the ratio of drug: stabilizer: co-stabilizer (PEG400) was equal to (1:8:2.5), and the stabilizer was Soluplus®. And the EE of our formulas ranges from 92% to 96%. The kind and concentration of the stabilizer greatly influence the goal of substantial drug entrapment efficiency.

Table 5: Drug content and EE of BF nanosuspension formulas

Formula code	Ratio of drug: stabilizer: co-stabilizer (PEG400)	Type of stabilizer	Drug content%±SD	EE%±SD
F4	1:3:3	Soluplus®	95.15±0.001	93±0.014
F7	1:3:1.5	Soluplus®	90.6±0.01	92±0.001
F8	1:3:2.5	Soluplus®	93.1±0.002	94±0.001
F13	1:8:2.5	Soluplus®	99.6±0.013	96±0.012
F18	1:8:1	Soluplus®	97.4±0.011	95±0.013

n = 3

Releasing the efficiency of butenafine HCL nanosuspensions

The release profile is an essential parameter for predicting the bioavailability of a drug from various formulations. The drug release profiles of the nanosuspension are shown in fig. 2. The similarity factor *f2* determines the degree of similarity in dissolution percentage, where the powder of Butenafine, utilized as a reference, is. The similarity in the dissolution percentage between optimum formulas shows a similar release profile between them, and there is a significant difference with the pure drug, which was found to be 34% after 120 min ±1 min, which differs from the optimum formula, which exceeds 90% after 120 min.

Differential scanning calorimetric

The DSC thermograms of Butenafine are presented in fig. 4, which shows a sharp endothermic peak at 218 °C. The thermogram of F15, an optimized formula, shows a slight shift in the melting point to 220.50 °C due to the presence of cryoprotectants fig. 5.

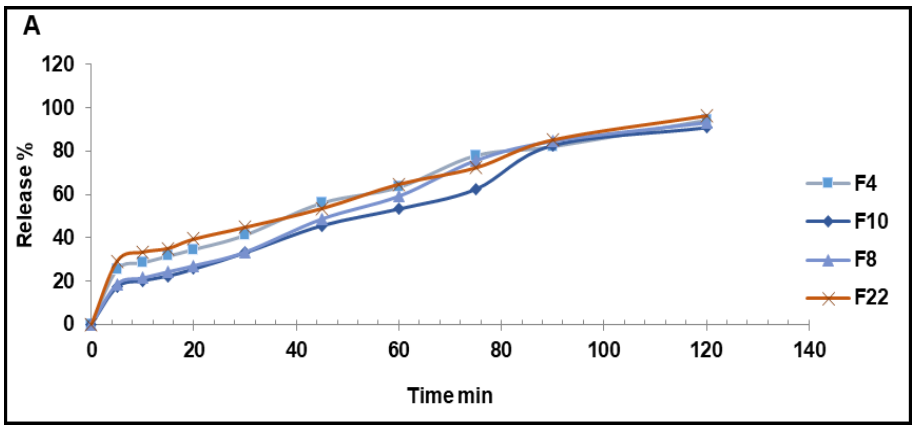

Fig. 3: (A) Release profile of nanosuspension formulas

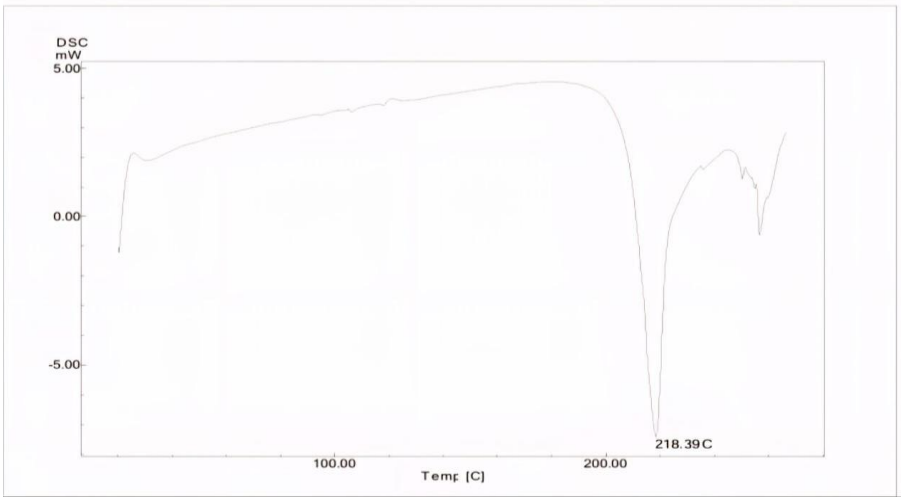

Fig. 4: DSC thermogram of butenafine HCL

Table 6: Similarity test results of butenafine HCL nanosuspension

Formula code	Zero order		First order		Higuchi		First order with Fmax		
	K_0	R_{seq}	K_1	R_{seq}	KH	R_{seq}	K_1	Rseq	F max
F4	0.858	0.9077	0.9563	0.015	7.495	0.9460	0.011	0.9631	123.562
F8	0.951	0.7385	0.9428	0.020	8.511	0.9863	0.022	0.9436	96.283
F13	0.915	0.8934	0.9648	0.017	8.019	0.9542	0.013	0.9721	119.812
F18	0.962	0.6389	0.8894	0.021	8.674	0.9756	0.026	0.8944	91.410

Table 7: Release kinetic parameter of butenafine HCL nanosuspension

Formula	F_2 value	Formula	F_2 value	Formula	F_2 value
Pure drug vs F4	41	Pure drug vs F18	29	F18vs F13	50
Pure drug vs F13	32	F4 vs F13	58		
Pure drug vs F8	40	F8 vs F13	89		

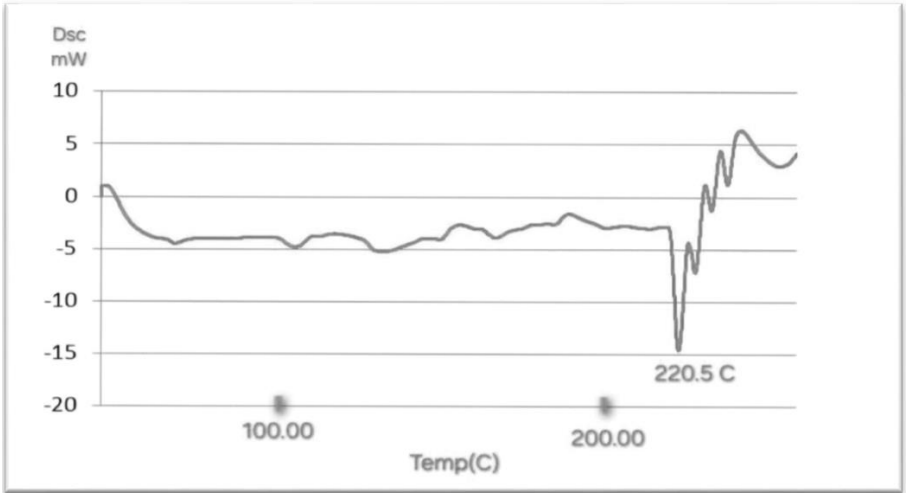

Fig. 5: DSC thermogram of F13 butenafine HCL nanosuspension

Powder X-ray diffraction (PXRD)

Pure butenafine HCL showed a sharp peak, which is indicative of its crystalline nature. The peaks at typical diffraction peaks of Butenafine HCL were observed at 5◦ to 60◦ (2θ) [50]. As shown in fig. 6. There were no typical crystal peaks of Butenafine. It can be concluded that Butenafine HCl was encapsulated in a polymeric nanosuspension in an amorphous state rather than as the free crystal drug, as shown in fig. 7. Fig. 8 shows Butenafine-soluplus® and the PEG physical mixture.

Fourier transform infrared spectroscopy (FTIR)

The pure butenafine HCL showed a sharp stretching CH2 peak at 2955.74 cm^{-1}, C–CH3 peaks at 2892.39 cm^{-1}, C=C aromatic peak at 1650.84 cm^{-1}, and C–N stretching peaks at1216.77 cm^{-1}[51] As shown in fig. 9. Fig. (10) FTIR of the BF nanosuspension formula showed no new peaks, revealing that there was interaction between the formulation ingredients and no structural or functional changes in the formulation.

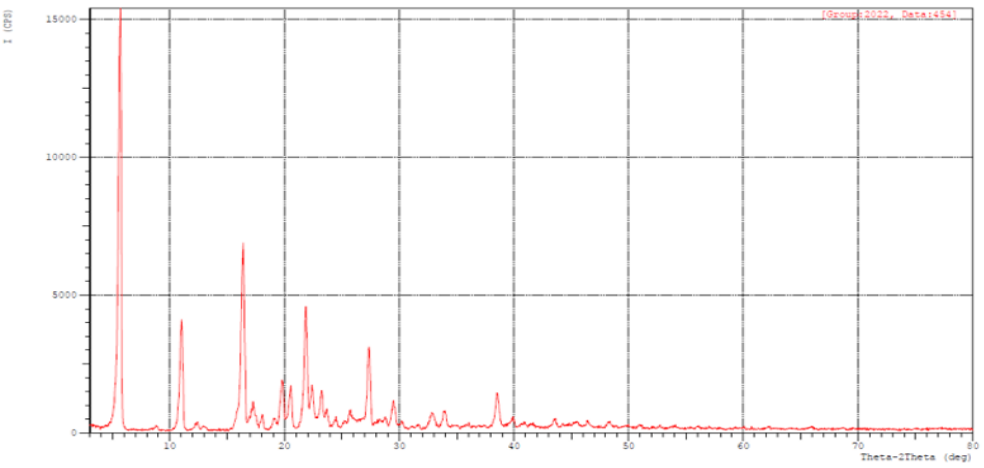

Fig. 6: Powder X-ray diffraction (PXRD) of pure drug

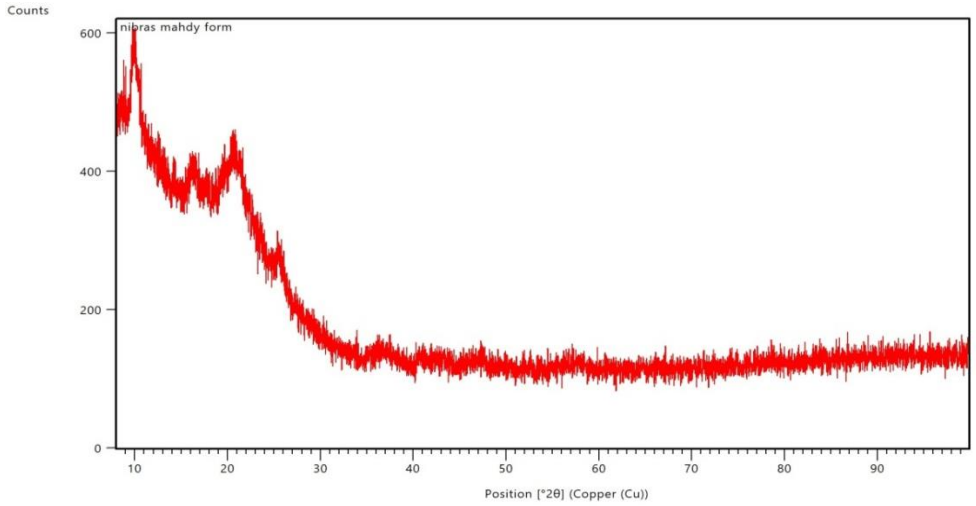

Fig. 7: Powder X-ray diffraction (PXRD) of F15 butenafine HCL nanosuspension

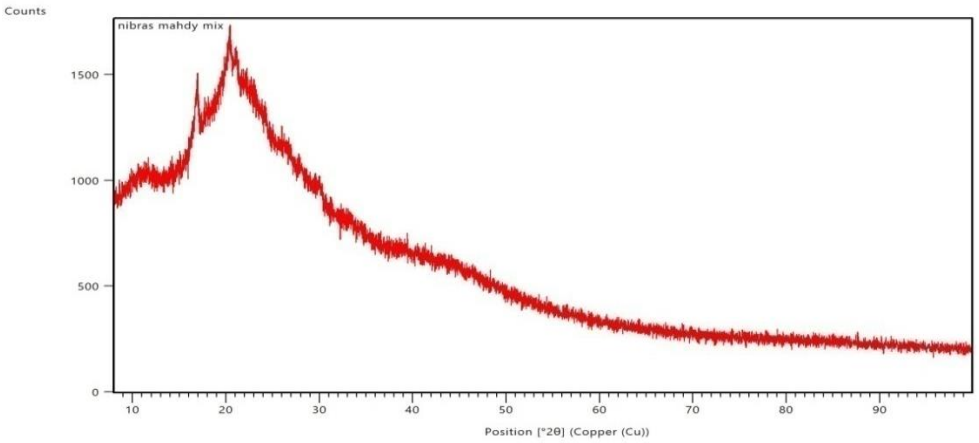

Fig. 8: Powder X-ray diffraction (PXRD) of physical mixture

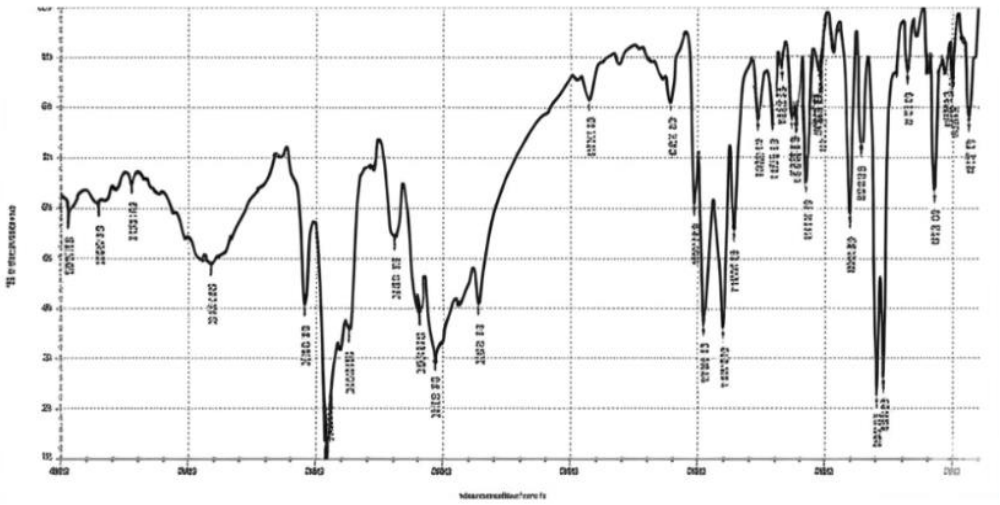

Fig. 9: Fourier transform infrared spectroscopy (FTIR) of pure Butenafine HCL

Field emission-scanning electron microscope (FESEM)

Images of the optimized formulation suggested that the formulations were in the nano-size range. FESEM images of the optimum formula showed that the developed nanoparticles are spherical in shape, as shown in fig. 12. The particles were found to be in the nano range, spherical in shape, and evenly distributed.

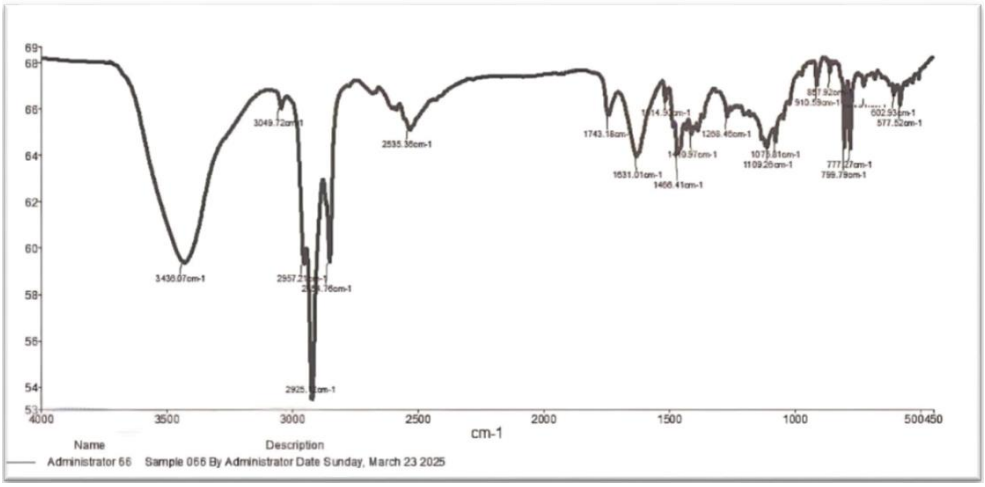

Fig. 10: Fourier transform infrared spectroscopy (FTIR) of F13 Butenafine HCL nanosuspension

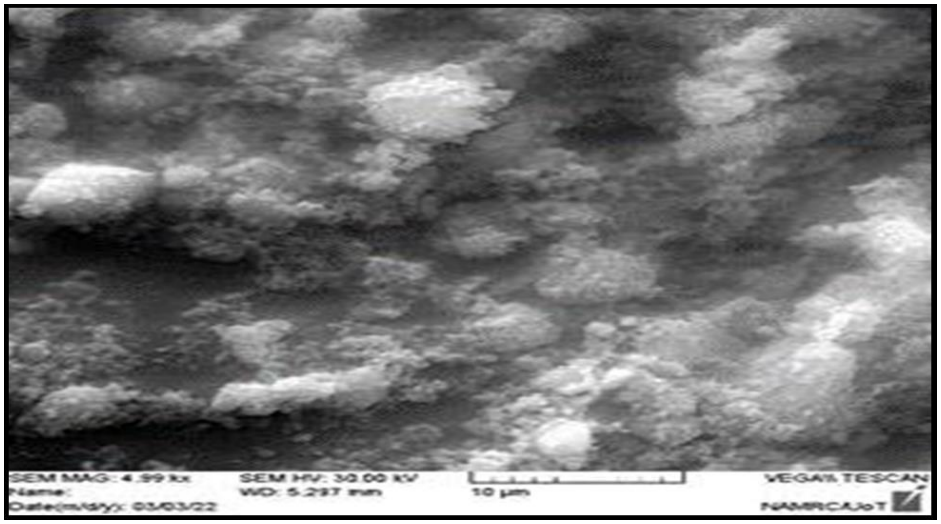

Fig. 11: FESEM of pure Butenafine HCL

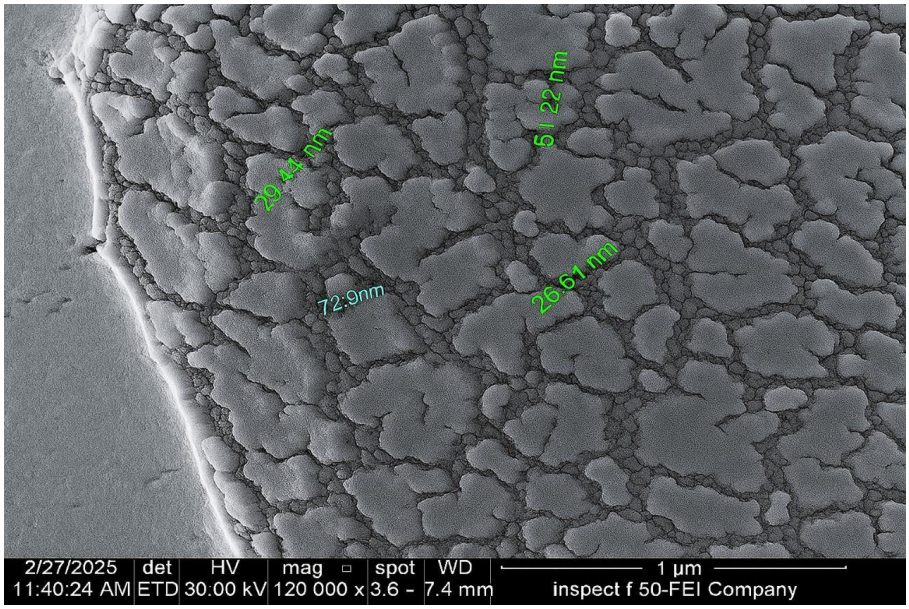

Fig. 12: FESEM of F13 butenafine HCL nanosuspension (magnification 120X)

Table 8: Stability parameter of F13 nanosuspension

Storage condition	PS (nm)	PDI	EE%	DRUG CONTENT %
5 °C After 3 mo	78 nm	0.25	96±3.6	99.1%
25 °C after 3 mo	80 nm	0.39	95.5± 2.4	97%

Data are given as mean±SD; n = 3

Osmolarity

Osmolarity is adjusted to a range of 280 to 310 mOsm/kg.

Sterility and lyophilized powder

Sterility testing was performed using membrane filtration to dilute the final formula serially. The lyophilized powder was sticky due to the presence of polyethylene glycol, which was used for the characterization of the optimal formula (DSC and PXRD).

Stability test

The result of the stability study is shown in table 8.

CONCLUSION

The objective of the current study was to formulate a nanosuspension of Butenafine HCl. These nanosuspensions have potential as drug delivery systems because they are highly biocompatible and exhibit relatively high stability, in addition to their capacity for controlled and targeted release profiles. They have attracted considerable interest in the cosmetic and pharmaceutical industries for improving the encapsulation efficiency and bioavailability of active substances. The nanosuspensions were also prepared at different surfactant concentrations, and polyethylene glycol was added as a cosurfactant. We found that the use of Soluplus® as a stabilizer at various concentrations successfully prepared Butenafine HCl nanosuspensions with nanoscale particle sizes. The optimum formula containing (Butenafine HCl-Soluplus®-PEG400 1-8-2.5) produces nanoparticles with a size of 78 nm, and a PDI value of 0.28 is obtained. This formulation enhanced the dissolution rate of Butenafine to a greater extent than that of the pure drug. We plan to prepare it as an ophthalmic in situ gel in our subsequent studies.

FUNDING

Nil

AUTHORS CONTRIBUTIONS

Nibras Mahdi Naeem designed and conceptualized the work performed and analyzed the data. Omar Saeb Salih-Analysis of the data and management of experimental work.

CONFLICT OF INTERESTS

Declared none

REFERENCES

1. Moskaluk AE, Vande Woude S. Current topics in dermatophyte classification and clinical diagnosis. Pathogens. 2022;11(9):957. doi: 10.3390/pathogens11090957, PMID 36145389.
2. Khan SS, Hay RJ, Saunte DM. A review of antifungal susceptibility testing for dermatophyte fungi and it's correlation with previous exposure and clinical responses. J Fungi (Basel). 2022;8(12):1290. doi: 10.3390/jof8121290, PMID 36547624.
3. Jain S, Kabi S, Swain B. Current trends of dermatophytosis in eastern Odisha. J Lab Physicians. 2020;12(1):10-4. doi: 10.1055/s-0040-1713063, PMID 32792788.
4. Trypanosomosis A, Transcriptomics S, Choi B, Vu HT, Vu HT, Radwanska M. Advances in the immunology of the host–parasite interactions in African trypanosomosis including single-cell transcriptomics. Pathogens. 2024;13(3):188. doi: 10.3390/pathogens13030188.
5. Awad R, Ghaith AA, Awad K, Mamdouh Saad MM, Elmassry AA. Fungal keratitis: diagnosis, management and recent advances. Clin Ophthalmol. 2024 Jan;18:85-106. doi: 10.2147/OPTH.S447138, PMID 38223815.
6. Ghenciu LA, Faur AC, Bolintineanu SL, Salavat MC, Maghiari AL. Recent advances in diagnosis and treatment approaches in fungal keratitis: a narrative review. Microorganisms. 2024;12(1):161. doi: 10.3390/microorganisms12010161, PMID 38257986.
7. Gaidhani KA, Harwalkar M, Bhambere D, Nirgude PS. Lyophilization/freeze drying-a review. World Journal of Pharmaceutical Research Formulation. 2021;2(5):1685-703.
8. Pınar SG, Oktay AN, Karakucuk AE, Celebi N. Formulation strategies of nanosuspensions for various administration routes. Pharmaceutics. 2023;15(5):1520. doi: 10.3390/pharmaceutics15051520, PMID 37242763.
9. Aldeeb MM, Wilar G, Suhandi C, Elamin KM, Wathoni N. Nanosuspension-based drug delivery systems for topical applications. Int J Nanomedicine. 2024;19:825-44. doi: 10.2147/IJN.S447429, PMID 38293608.
10. Tarivitla LP, Sunitha Reddy M. An overview of the biopharmaceutics classification system (BCS). GSC Biol Pharm Sci. 2021;14(2):217-21. doi: 10.30574/gscbps.2021.14.2.0012.
11. Bezerra Souza A, Fernandez Garcia R, Rodrigues GF, Bolas Fernandez F, Dalastra Laurenti MD, Passero LF. Repurposing butenafine as an oral nanomedicine for visceral leishmaniasis. Pharmaceutics. 2019;11(7):353. doi: 10.3390/pharmaceutics11070353, PMID 31330776.
12. Bezerra Souza A, Jesus JA, Laurenti MD, Lalatsa A, Serrano DR, Passero LF. Nanoemulsified butenafine for enhanced performance against experimental cutaneous leishmaniasis. J Immunol Res. 2021;2021:8828750. doi: 10.1155/2021/8828750, PMID 33880383.
13. Mahdi WA, Bukhari SI, Imam SS, Alshehri S, Zafar A, Yasir M. Formulation and optimization of butenafine loaded topical nano lipid carrier-based gel: characterization, irritation study and anti-fungal activity. Pharmaceutics. 2021;13(7):1087. doi: 10.3390/pharmaceutics13071087, PMID 34371777.
14. Kumar S, Naved T, Alam S, Chauhan R. Design and optimization of telmisartan nanosuspension for improved drug delivery. Biochem Cell Arch. 2023;23(2):925-31. doi: 10.51470/bca.2023.23.2.925.
15. Gulbag Pınar S, Celebi N. Development of cyclosporine a nanosuspension using experimental design by response surface methodology: *in vitro* evaluations. Turk J Pharm Sci. 2024;21(5):428-39. doi: 10.4274/tjps.galenos.2023.68054.
16. Sopyan I, Gozali D, Sriwidodo, Guntina RK. Design-expert software (DOE): an application tool for optimization in pharmaceutical preparations formulation. Int J App Pharm. 2022;14(4):55-63. doi: 10.22159/ijap.2022v14i4.45144.
17. Alwan ZS. Preparation and characterization of febuxostat as nanosuspension. Iraqi J Pharm Sci. 2025;33(13):261-70. doi: 10.31351/vol33iss(4SI)pp261-270.
18. Ugur Kaplan AB, Ozturk N, Cetin M, Vural I, Oznuluer Ozer TO. The nanosuspension formulations of daidzein: preparation and *in vitro* characterization. Turk J Pharm Sci. 2022;19(1):84-92. doi: 10.4274/tjps.galenos.2021.81905, PMID 35227054.
19. Bellouniversity A. Formulation and *in vitro* evaluation of sustained release. J Pharm Sci Innov. 2013;12(1):1-5.
20. Wang D, Qian J, He S, Park JS, Lee KS, Han S. Aggregation-enhanced fluorescence in pegylated phospholipid nanomicelles for *in vivo* imaging. Biomaterials. 2011;32(25):5880-8. doi: 10.1016/j.biomaterials.2011.04.080, PMID 21601279.
21. Al wiswasi NN, Al Gawahri FJ. Brimonidine-soluplus nanomicelles: preparation and *in vitro* evaluation. Iraqi J Pharm Sci. 2025;34(1):246-55. doi: 10.31351/vol34iss1pp246-255.
22. Sumathi R, Tamizharasi S, Sivakumar T. Formulation and evaluation of polymeric nanosuspension of naringenin. Int J App Pharm. 2017;9(6):60-70. doi: 10.22159/ijap.2017v9i6.21674.

23. Rashid AM, Ghareeb MM. Using ionic liquids-based surfactant in formulating nimodipine polymeric nanoparticles: a promising approach for improved performance. Iraqi J Pharm Sci. 2025;34(1):203-17. doi: 10.31351/vol34iss1pp203-217.
24. Khaira R, Sharma J, Saini V. Development and characterization of nanoparticles for the delivery of gemcitabine hydrochloride. Scientific World Journal. 2014;2014:560962. doi: 10.1155/2014/560962, PMID 24592173.
25. Al Edhari GH, Al Gawhari FJ. Study the effect of formulation variables on preparation of nisoldipine-loaded nanobilosomes. IJPS. 2023;32(Suppl):271-82. doi: 10.31351/vol32issSuppl.pp271-282.
26. Alsafar ZA, Jawad FJ. Preparation and evaluation of lercanidipine HCl nanosuspension to improve the dissolution rate. Iraqi J Pharm Sci. 2024;33(4SI):20-30. doi: 10.31351/vol33iss(4SI)pp20-30.
27. Keshari P, Sonar Y, Mahajan H. Curcumin-loaded TPGS micelles for nose-to-brain drug delivery: *in vitro* and *in vivo* studies. Mater Tech. 2019;34(7):423-32. doi: 10.1080/10667857.2019.1575535.
28. Salamanca CH, Barrera Ocampo A, Lasso JC, Camacho N, Yarce CJ. Franz diffusion cell approach for pre-formulation characterisation of ketoprofen semi-solid dosage forms. Pharmaceutics. 2018;10(3):148. doi: 10.3390/pharmaceutics10030148, PMID 30189634.
29. Costa P, Sousa Lobo JM. Modeling and comparison of dissolution profiles. Eur J Pharm Sci. 2001;13(2):123-33. doi: 10.1016/S0928-0987(01)00095-1, PMID 11297896.
30. Anusha G, Sunayana R, Ponnam M, Kumar BA. The application of marine natural products (MNPS) in anti-COVID-19 therapeutics. Asian Journal of Pharmaceutical Research and Development. 2020;8(6):77-80. doi: 10.22270/ajprd.v8i6.809.
31. Salih OS, Jaber SA, Sulaiman HT. Ultra HPLC method development and validation for the determination of meclizine in pharmaceutical formulation. J Adv Pharm Educ Res. 2025;15(3):69-76. doi: 10.51847/3Wcyztstn0.
32. Salih OS. Study the sustained release effect of different polymers used in the formulation of aspirin-rosuvastatin tablets. Int J Pharm Pharm Sci. 2015;7(12):166-72.
33. Hussein AA, Samein LH, Ghareeb MM, Salih OS. Effects of mucoadhesive polymers combination on the properties of lisinopril buccal tablets prepared by the wet granulation method. Int J Pharm Pharm Sci. 2013;5(4):340-3.
34. Bhosale VA, Srivastava V, Valamla B, Yadav R, Singh SB, Mehra NK. Preparation and evaluation of modified chitosan nanoparticles using anionic sodium alginate polymer for treatment of ocular disease. Pharmaceutics. 2022;14(12):2802. doi: 10.3390/pharmaceutics14122802.
35. Tomlinson A, Khanal S, Ramaesh K, Diaper CJM, McFadyen A. Tear film osmolarity: determination of a referent for dry eye diagnosis. Invest Ophthalmol Vis Sci. 2006;47(10):4309–15. doi: 10.1167/iovs.05-1504.
36. Mastiholimath VS, Rajendra BA, Mannur VS, Dandagi PM, Gadad AP, Khanal P. Formulation and evaluation of cefixime nanosuspension for the enhancement of oral bioavailability by solvent-antisolvent method and its suitable method development. Indian J Pharm Educ Res. 2019;54(1):55-67. doi: 10.5530/ijper.54.1.7.
37. Abbas IK, Rajab NA, Hussein AA. Formulation and *in vitro* evaluation of darifenacin hydrobromide as buccal films. Iraqi J Pharm Sci. 2019;28(2):83-94. doi: 10.31351/vol28iss2pp83-94.
38. Thamer AK, Abood AN. Preparation and *in vitro* characterization of aceclofenac nanosuspension (ACNS) for enhancement of percutaneous absorption using hydrogel dosage form. Iraqi J Pharm Sci. 2021;30(2):86-98. doi: 10.31351/vol30iss2pp86-98.
39. Gupta AK, Madan S, Majumdar DK, Maitra A. Ketorolac entrapped in polymeric micelles: preparation, characterisation and ocular anti-inflammatory studies. Int J Pharm. 2000;209(1-2):1-14. doi: 10.1016/S0378-5173(00)00508-1, PMID 11084241.
40. Rashid AM, Abdal Hammid SN. Formulation and characterization of itraconazole as nanosuspension dosage form for enhancement of solubility. Iraqi J Pharm Sci. 2019;28(2):124-33. doi: 10.31351/vol28iss2pp124-133.
41. Khafeef HK, Rajab NA. Eplerenone crystal nanosuspension for solubility enhancement: preparation and evaluation. Maaen J Med Sci. 2023;2(2):73-80. doi: 10.55810/2789-9136.1024.
42. Ubgade S, Bapat A, Kilor V. Effect of various stabilizers on the stability of lansoprazole nanosuspension prepared using high shear homogenization: preliminary investigation. J Appl Pharm Sci. 2021;11(9):85-92. doi: 10.7324/JAPS.2021.110910.
43. Patil AS, Hegde R, Gadad AP, Dandagi PM, Masareddy R, Bolmal U. Exploring the solvent-anti-solvent method of nanosuspension for enhanced oral bioavailability of lovastatin. Turk J Pharm Sci. 2021;18(5):541-9. doi: 10.4274/tjps.galenos.2020.65047, PMID 34708645.
44. Ma Y, Cong Z, Gao P, Wang Y. Nanosuspensions technology as a master key for natural products drug delivery and *in vivo* fate. Eur J Pharm Sci. 2023;185:106425. doi: 10.1016/j.ejps.2023.106425.
45. Ismanelly Hanum TI, Nasution A, Sumaiyah S, Bangun H. Physical stability and dissolution of ketoprofen nanosuspension formulation: polyvinylpyrrolidone and Tween 80 as stabilizers. Pharmacia. 2023;70(1):209-15. doi: 10.3897/pharmacia.70.e96593.
46. Elmowafy M, Shalaby K, Al Sanea MM, Hendawy OM, Salama A, Ibrahim MF. Influence of stabilizer on the development of luteolin nanosuspension for cutaneous delivery: an *in vitro* and *in vivo* evaluation. Pharmaceutics. 2021;13(11):1812. doi: 10.3390/pharmaceutics13111812, PMID 34834227.
47. Guembe Michel N, Nguewa P, Gonzalez Gaitano G. Soluplus®-based pharmaceutical formulations: recent advances in drug delivery and biomedical applications. Int J Mol Sci. 2025;26(4):1499. doi: 10.3390/ijms26041499, PMID 40003966.
48. Alwan RM, Rajab NA. Nanosuspensions of selexipag: formulation characterization and *in vitro* evaluation. Iraqi J Pharm Sci. 2021;30(1):144-53. doi: 10.31351/vol30iss1pp144-153.
49. Touqeer SI, Jahan N, Abbas N, Ali A. Formulation and process optimization of rauvolfia serpentina nanosuspension by HPMC and *in vitro* evaluation of ACE inhibitory potential. J Funct Biomater. 2022;13(4):268. doi: 10.3390/jfb13040268, PMID 36547528.
50. Lu P, Liang Z, Zhang Z, Yang J, Song F, Zhou T. Novel nanomicelle butenafine formulation for ocular drug delivery against fungal keratitis: *in vitro* and *in vivo* study. Eur J Pharm Sci. 2024;192:106629. doi: 10.1016/j.ejps.2023.106629, PMID 37918544.